Study of Photoacoustic Effect in Solids and Liquids

Sohair Negm

Department of Mathematics and Physics, Faculty of Engineering (Shoubra) Zagazig University (Benha), and Advanced Laser Spectroscopy Lab., Faculty of Science, Ain Shams University.

The principle and practice of Photoacoustic Spectroscopy is given. The theoretical formulation follows Rosencwaig in considering the solid undergoing periodic absorption of light acts as a piston in the surrounding gas. Data for photoacoustic spectroscopy for solids in powder form and for solutions of dyes of different concentration are shown to be a good representation of the optical absorption of the material. The dependence of the photoacoustic signal on the experimental conditions e.g. the chopping frequency of light is also given.

1-Introduction:

Photoacoustic (PA) spectroscopy [1-8] is a technique for the study of optical absorption spectra directly. The basic idea of the method is to place the sample to be investigated in a closed cell containing a gas or air and a sensitive microphone. The sample is illuminated by light that is modulated or chopped at audio frequencies. The sample undergoes optical absorption at the surface and is heated through nonradiative transitions and the heat is transferred to the gas in the cell. Since the sample heating is modulated, the gas heating produces a pressure fluctuation within the cell which can be detected by the microphone as an acoustic signal. The analog signal from the microphone is then phase sensitively detected. The resulting PA signal depends not only on the amount of heat generated by the sample, but also on the way heat diffuses through the sample. There are two modes of operation in these experiments. In the first, the light is chopped at a constant frequency, and the incident wavelength is varied. In the second, the light wavelength is kept constant and the chopping frequency is varied. PA spectroscopy discovered by Tyndall [9] and Roentgen [10] and later was developed by Rosencwaig [11]. The PA technique has many advantages: i) It enables one to obtain spectra similar to optical absorption spectra on any type of solids or semisolid materials, whether it be crystalline, powder, amorphous, smear, gel, etc. This capability is based on the fact that only the absorbed light is converted into sound. ii) Scattered light, which presents serious problem when dealing with many solid materials by conventional spectroscopic techniques, presents no difficulties in photoacoustic spectroscopy. iii) It has been found experimentally that good optical absorption data can be obtained, with the photoacoustic technique, on materials that are completely opaque to transmitted light [1]. iv) Photoacoustic spectroscopy has already found some important applications in research and analysis of inorganic, organic and biological solids and semisolids [12-13]. v) Furthermore, it has very strong potential as spectroscopic technique not only in the study of bulk optical properties, but also in surface studies and deexcitation studies [1].

Because of the above advantages of PA spectroscopy, it was decided to initiate such spectroscopy and to construct the experimental set-up of the PA technique at the Laser Laboratory at Ain Shams University. In the following we present a formulation of the principles of PA techniques along lines similar to but not identical to those followed by Rosencwaig and Gersho (RG) [14, 15].

2- Theory:

The standard theory of photoacoustic effect with solids developed in a classic paper by RG [14,15], where, they formulate a one dimensional model of the heat flow in the cell resulting from the absorbed light energy. However in this paper the theory of PA that is developed independently and the resulting expression have a close resemblance to RG results. This section is divided into three subsections to present first; the heat flow through the sample, second; the temperature distribution in the PA cell and third; the production of the PA signal.

i- Heat- flow equations

Consider a simple cylindrical cell (as shown in Fig.1) of diameter D and length $L = \ell + \ell_b + \ell_g$, where ℓ is the length of the sample, ℓ_b is the length of a poor thermal conducting backing material and ℓ_g is the length of the gas column in the cell. Assuming that the gas and backing materials are not light absorbing and a sinusoidally chopped monochromatic light with wavelength λ is incident on the solid with intensity $I = I_o (1 + \cos \omega t) / 2$ where I_o is the incident monochromatic light flux and ω is the chopping frequency. The following parameters are defined: K_i, the thermal conductivity of material i (cal/cm.sec.K); ρ_i, the density of material i (g/cm^3); c_i, the specific heat of material i (cal/g.K); $\alpha_i = K_i/\rho_i c_i$, the diffusivity of material i; $a_i = (\omega/2\alpha_i)^{1/2}$ where the subscripts i = s, g or b denote the sample, gas or backing material respectively. Let $\phi_i (x, t)$ denote the temperature in material i relative to ambient temperature (T_o) due to light into heat conversion process. By neglecting the heat losses by radiation at the lateral surfaces, the temperature in the cell obeys the thermal diffusion equations as those of RG theory [14].

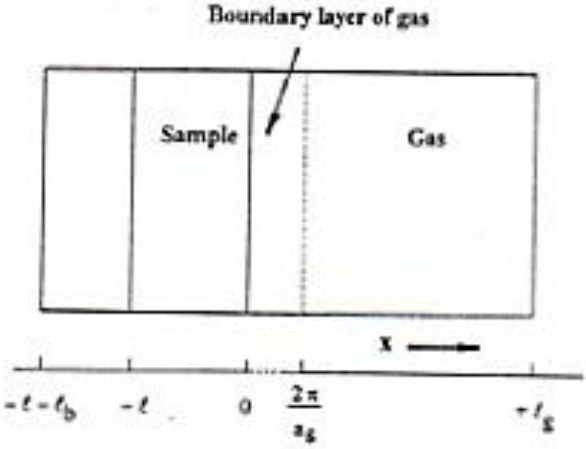

Fig.1 Schematic configuration of the photoacoustic cell.

The thermal diffusion equation in the solid taking into account the distributed heat source can be written as

$$\frac{\delta^2\Phi_s}{\delta x^2} = \frac{1}{\alpha_s}\frac{\delta\Phi_s}{\delta t} - A\exp(\beta x)[1+\exp(i\omega t)] \qquad -\ell \le x \le 0 \quad (1)$$

where β is the optical absorption coefficient of the solid sample (in cm^{-1}) for the wavelength λ, $A = \beta I_o \eta K_s$, where η is the efficiency at which the absorbed light at wavelength λ, is converted to heat by the nonradiative deexcitation processes. Assuming $\eta = 1$ which is reasonable for most solids at room temperature. For the backing and the gas, the heat diffusion equations are given by

$$\frac{\delta^2\Phi_b}{\delta x^2} = \frac{1}{\alpha_b}\frac{\delta\Phi_b}{\delta t} \qquad -\ell-\ell_b \le x \le -\ell \quad (2)$$

$$\frac{\delta^2\Phi_g}{\delta x^2} = \frac{1}{\alpha_g}\frac{\delta\Phi_g}{\delta t} \qquad 0 \le x \le \ell_g \quad (3)$$

The real part of the complex-valued ϕ_i (x, t) is, of course, the solution of physical interest. This, in turn, is obtained by solving the thermal diffusion equations together with the appropriate boundary conditions requiring the temperature and heat-flux continuity at the boundaries $x = 0$ and $x = -\ell$, together with the constraint that the temperature at the cell walls is at ambient temperature [i.e. $\phi_g(-\ell_g) = \phi_b(-\ell - \ell_b) = 0$]. It could be argued that the transition from the sample to the gas involves not only a discontinuity in the derivatives but also in the temperature itself due to the surface layer with a nonzero surface thermal resistance. Such surface effects may be important if the length of the heat transfer into the gas becomes comparable to the gas thermal diffusion length $(2\alpha_g/\omega)^{1/2}$.

ii- Temperature Distribution in the cell

To solve the above equations for $\Phi(x, t)$ in the cell, we use the method of separation of variables. This method cannot be used directly here since the boundary conditions are non-homogeneous. To analyse this problem, we first obtain an equilibrium temperature distribution $\phi(x)$. This temperature must satisfy the steady-state (time independent equation)

$$\frac{d^2\phi}{dx^2} = 0 \qquad \text{at no source}$$

and

$$\frac{d^2\phi}{dx^2} = f(x) \qquad \text{where } f(x) \text{ is the source}$$

Applying this role to the equations (1) - (3) so the dc components of the temperature can be written as

$$\phi_g(x) = (1-\frac{x}{\ell_g})\,\theta_0$$

$$\phi_b(x) = \frac{1}{\ell_b}(x+\ell+\ell_b)\,W_o \qquad (4)$$

$$\phi_s(x) = e_1 + e_2 x + d\exp(\beta x)$$

where θ_o, W_o, e_1, e_2 and d are real valued constants. The dc solution in the backing and gas already make use of the assumption that the temperature (relative to ambient) is zero at the ends of the cell. The quantities W_o and θ_o denote the dc component of the temperature (relative to ambient) at the sample surfaces $x = -\ell$ and $x = 0$, respectively. The quantity d is determined by the forcing function in equation (1) $d = -A/\beta^2$.

Then consider the temperature variation from the equilibrium temperature

$$v(x,t) = \Phi(x,t) - \phi(x)$$

such that

$$\frac{\partial^2 v(x,t)}{\partial x^2} = \frac{1}{\alpha}\frac{\partial v(x,t)}{\partial t} + f(x,t)$$

i.e. v(x, t) satisfy the diffusion equations.

To find v(x, t), consider $v(x, t) = v(x)\,e^{i\omega t}$, then substitute with v(x, t) into the diffusion equations in the three media. The ac components of the temperature can be written as

$$V_g(x,t) = \theta \exp(-\sigma_g x + i\omega t)$$

$$V_b(x,t) = W \exp[\sigma_b(x+\ell) + i\omega t] \qquad (5)$$

$$V_s(x,t) = [U \exp(\sigma_s x) + Z \exp(-\sigma_s x) - E \exp(\beta x)]\, e^{i\omega t}$$

where θ, W,U,Z and E are complex-valued constants. In particular, it should be noted that θ and W represent the complex amplitudes of the periodic temperatures at the sample-gas boundary ($x = 0$) and the sample backing ($x = -\ell$), respectively. The quantity E determined by the forcing function in (1)

$$E = \frac{A}{\beta^2 - \sigma^2} = \frac{\beta I_o}{2K_s(\beta^2 - \sigma_s^2)}$$

In the ac solution, equation(5), we have omitted the growing exponential component of the solutions to the gas and backing material where this solution is not accepted physically. Combining equations (4) and (5), we get the general solution of equations (1)-(3)

$$\Phi(x,t) = \frac{1}{\ell_b}(x+\ell+\ell_b)W_0 + W\exp[\sigma_b(x+\ell)+i\omega t] \qquad -\ell-\ell_b \le x \le -\ell$$

$$= e_1 + e_2 x + d\exp(\beta x) + [U\exp(\sigma_s x) + Z\exp(-\sigma_s x) - E\exp(\beta x)]\exp(i\omega t) \qquad -\ell \le x \le 0$$

$$= (1 - \frac{x}{\ell_g})\theta_o + \theta\exp(-\sigma_g x + i\omega t) \qquad 0 \le x \le \ell$$

(6)

The temperature and heat flux continuity conditions at the sample surfaces are explicitly given by

$$\Phi_g(0,t) = \Phi_s(0,t)$$

$$\Phi_b(-\ell,t) = \Phi_s(-\ell,t)$$

$$K_g \frac{\partial \Phi_g}{\partial x}(0,t) = K_s \frac{\partial \Phi_s}{\partial x}(0,t) \qquad (7)$$

and $$K_b \frac{\partial \Phi_b}{\partial x}(-\ell,t) = K_s \frac{\partial \Phi_s}{\partial x}(-\ell,t)$$

where the subscripts s, b and g identify the solution in equation (6) for the temperature in the solid, backing and gas, respectively. These constraints apply separately to the dc component and the sinusoidal component of the solution. Applying equations (7) to the sinusoidal component of the solution yields

$$\theta = U + Z - E \qquad (8\text{-a})$$

$$W = U\exp(-\sigma_s \ell) + Z\exp(\sigma\ell) - E\exp(-\beta\ell) \qquad (8\text{-b})$$

$$g\theta = -U + Z + rE \qquad (8\text{-c})$$

$$bW = U\exp(-\sigma\ell) - Z\exp(\sigma\ell) - r\,E\exp(-\beta\ell) \qquad (8\text{-d})$$

where $r = (1-i)\frac{\beta}{2a_s} = \frac{\beta}{\sigma_s}$, $g = \frac{k_g a_g}{k_s a_s}$ and $b = \frac{k_b a_b}{k_s a_s}$

From equation (7), we obtain the dc components of the solution

$$\theta_o = c_1 + d$$

$$W_o = e_1 - e_2\ell + d\exp(-\beta\ell)$$

$$(-k_g/\ell_g)\theta_o = k_s e_2 + k_s\beta d \qquad (9)$$

$$(k_b/\ell_b)W_o = k_s e_2 + k_s\beta d\exp(-\beta\ell)$$

Equations (8) together with the expression for E determine the coefficients U, Z, W and θ. Hence the solution to equations (8) and (9) allow us to evaluate the temperature distribution, equations (1-3) in the cell in terms of optical, thermal, and geometric parameters of the system. We want to determine the explicit solution for θ, the complex amplitude of the periodic temperature at solid-gas boundary (x = 0). From equations (8-a) and (8-c)

$$U(g+1) + Z(g-1) - E(g+r) = 0 \qquad (10)$$

From equations (8-b) and (8-d)

$$U(b-1)\exp(-\sigma\ell) + Z(b+1)\exp(\sigma\ell) + E(r-b)\exp(-\beta\ell) = 0 \qquad (11)$$

From equation (10)

$$U = \frac{E(g+r) - Z(g-1)}{g+1} \qquad (12)$$

Substitute with U into equation (11)

$$Z = E\,\frac{(b-1)(g+r)e^{-\sigma\ell} + (g+1)(r-b)e^{-\beta\ell}}{(b-1)(g-1)e^{-\sigma\ell} - (g+1)(b+1)e^{\sigma\ell}} \qquad (13)$$

Substitute with Z into equation (12)

$$U = E\,\frac{(g+1)(g-1)(b-r)e^{-\beta\ell} - (g+r)(g+1)(b+1)e^{\sigma\ell}}{(g+1)(b-1)(g-1)e^{-\sigma\ell} - (g+1)(b+1)(g+1)e^{\sigma\ell}} \qquad (14)$$

From equations (13) and (14), we can find θ

$$\theta = U + Z - E$$

$$\therefore\ \theta = \frac{\beta I_0}{2K_s(\beta^2-\sigma^2)}\ \frac{(r-1)(b+1)e^{\sigma\ell} - (r+1)(b-1)e^{-\sigma\ell} + 2(b-r)e^{-\beta\ell}}{(g+1)(b+1)e^{\sigma\ell} - (g-1)(b-1)e^{-\sigma\ell}} \qquad (15)$$

iii- Production of the acoustic signal

The main source of the acoustic signal arises from the periodic heat flow from the solid to the surrounding gas. The periodic diffusion process produces a periodic temperature variation in the gas given by the sinusoidal (ac) component of the solution

$$\Phi_{ac}(x,t) = \theta\exp(-\sigma_g x + i\omega t) \qquad (16)$$

At a distance of only $2\pi\mu_g$ the periodic temperature variation in the gas is effectively damped out. The spatially averaged temperature of the gas within this boundary layer as a function of time can be determined by evaluating

$$\overline{\Phi}(t) = \frac{1}{2\pi\mu_g}\int_0^{2\pi\mu_g}\phi_{ac}(x,t)\,dx \tag{17}$$

From equation (16), we find

$$\Phi(t) = \frac{\theta\, e^{i\omega t}}{2\pi\mu_g}\int_0^{2\pi\mu_g} e^{-\sigma_g x}\,dx$$

Then

$$\Phi(t) \cong \frac{\theta}{2\sqrt{2\pi}}\exp\left[i\left(\omega t-\frac{\pi}{4}\right)\right]$$

Because of the periodic heating of the boundary layer, this layer of gas expands and contracts periodically and thus can be thought of as acting as an acoustic piston on the rest of the gas column producing an acoustic pressure signal that travels through the entire gas column. The displacement of the gas piston can be simply estimated by using the ideal gas law.

$$\delta x(t) = 2\pi\mu_g\frac{\Phi(t)}{T_0}$$

If we assume that the rest of the gas responds adiabatically, then the acoustic pressure in the cell is also derived from the adiabatic gas law

$$PV^{\gamma} = \text{constant}$$

where P is the pressure, V the gas volume in the cell, and γ the ratio of the specific heat.

$$\delta p(t) = \frac{\gamma P_0}{v_0}\delta v = \gamma\frac{P_0}{\ell_g}\delta x(t)$$

Thus the incremental pressure is

$$\delta P(t) = Q\exp\left[i\left(\omega t-\frac{\pi}{4}\right)\right] \tag{18}$$

where $$Q = \frac{\gamma P_0\,\theta}{\sqrt{2}\,\ell_g a_g T_0}$$

Q specifies the complex envelope of the sinusoidal pressure variation.

$$Q = \frac{\beta I_0 \gamma P_0}{2\sqrt{2}\,k_s \ell_g a_g T_0(\beta^2-\sigma_s^2)}\left[\frac{(\gamma-1)(b+1)e^{\sigma_s\ell}-(\gamma+1)(b-1)e^{-\sigma_s\ell}+2(b-\gamma)e^{-\beta\ell}}{(g+1)(b+1)e^{\sigma_s\ell}-(g-1)(b-1)e^{-\sigma_s\ell}}\right]$$

(19)

Experimental Procedure:

A block diagram of the Photoacoustic spectrometer is given in Fig.(2). The light source is a 1000W tungsten-halogen lamp, with its housing cooled by water circulation and small air fan. The light from the lamp is focused by a glass lens L_1 into the entrance slit of the monochromator (Carl Zeiss Jena 287804) to provide a tunable light source. A mechanical chopper (variable speed) [15Hz-10KHz light chopper, Noise Interference Type Boston Electronic (617) 566-382] is located in front of the entrance slit of the monochromator. Its purpose is to interrupt the light beam and to provide the reference signal for detection. The monochromator is motorized to allow for accurate scan of the wavelength. The output light is focused on the sample inside the PA cell (Model 6003) by using a camera lens L_2. The signal from the PA cell is received with a Princeton Applied Research Model 186A Lock-in amplifier. The output from the Lock-in amplifier is recorded on a personal computer.

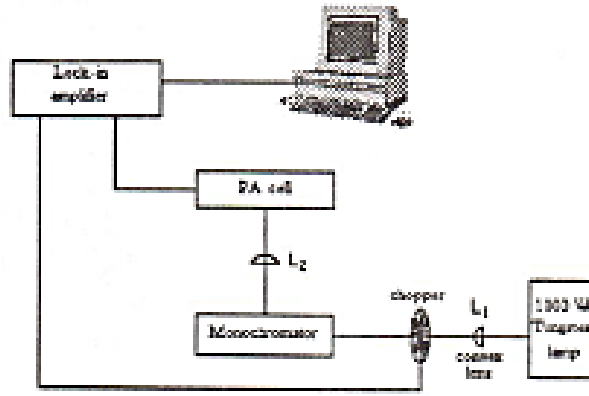

Fig.2 Experimental setup of the Photoacoustic (PAS) technique.

Model 6003 PA cell is designed for PAS application in both FT-IR and UV-VIS spectroscopy. Construction is of stainless steel and anodized aluminium and includes a built-in calibration microphone and preamplifier. The cell volume is 0.5 cubic cm. samples can be easily located and the sample cup is readily removable for cleaning or changing. The cell is designed for high signal-to noise ratios and acoustic vibration isolation. A series of right-angle bends in the channel that couples the sample volume to the microphone prevents coherent pickup from scattered light and protects the microphone from scattered light and protects the microphone from foreign matter or intrusions. The window of the sample carrier is available in several materials (2mm thick) to cover the UV-VIS-IR ranges. A 45° mirror mount, adjustable in height over a one-inch range, can be supplied for directing the beam into the sample chamber. Plane and spherical 25mm aluminium mirrors are available, with enhanced dielectric coatings. A separate unit, preamplifier/power supply, is also available to increase the signal to a level suitable for connection to the standard director input of most FT-IR's. The gain of the preamplifier is adjustable to allow for optimal signal levels. The PAS cell is sealed with rubber O-rings at the sample holder and microphone outlet. The cell is filled with air at room temperature and atmospheric pressure.

A few spectra are included here in this work to illustrate the operation of the setup the variation of the amplitude of the photoacoustic signal with the chopping frequency, and the dependence of the amplitude of the photoacoustic signal on the concentration of the liquid samples.

1- Photoacoustic measurements of Holmium Oxide Ho_2O_3

The selective sensitivity of the PAS technique to the non-radiative deexcitation channel can be used to great advantage in the study of fluorescent materials such as Ho_2O_3 particularly in the powder form where no other spectroscopic technique is possible.

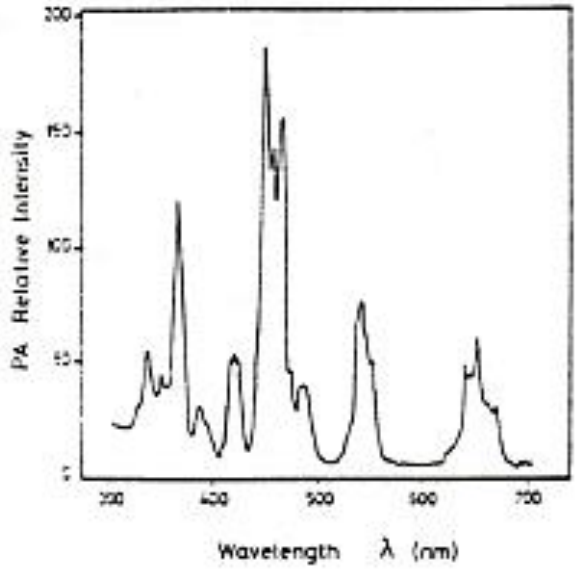

Fig.3 The normalized PA spectrum of holmium oxide Ho_2O_3 over the range of 350 to 700 nm - modulation frequency 20 Hz, time constant 1 sec.

Fig.(3) shows the normalized PA spectrum of holmium oxide Ho_2O_3 over the range of 350 to 700 nm, made with modulation frequency of 20 Hz and a time constant 1 sec. A 1128A holmium oxide 99.99% is in powder form and is simply placed in a sample holder. The reference signal is derived from carbon black sample. All of the lines present in this spectrum correspond to known Ho^{3+} energy levels the lines are nearly 350, 420, 470, 480, 530 and 640 nm.

When an optically excited energy level decays via fluorescence, then little or no acoustic signal will be produced in the PA cell. In the case of fluorescent materials, a combination of conventional fluorescence spectroscopy and PA spectroscopy will therefore provide data about both the radiative and non-radiative deexcitation processes within these solids. That is, the complete deexcitation process within these compounds can be readily studied. Since PAS spectroscopy gives phase as well as amplitude information, one can study exciton processes (random walk, lifetime, etc...) in these materials as a function of temperature and dopant concentration.

2- The photoacoustic spectra for dyes of different concentrations

We have employed the PAS technique to investigate PA signal of 3 dye materials having different absorption bands. These dyes are Rhodamine 6G (Rh6G), Rhodamine B (RhB) and cresyl violet (CV). The normalized spectra for the three dyes in their powder form can be seen in Figs.(4-a, b & c). The PAS spectra for Rh6G exhibits a peak at ≈ 560 nm, while in the case of RhB and CV, it exhibits peaks at ≈ 570 and ≈ 640 nm respectively which are in complete agreement with their optical absorption bands. Furthermore, we also employed the PA spectra to study the dependence of the PA signal on the concentration of the dyes in liquid form. The resulting PA spectra of different concentrations of Rh6G in ethanol as well as in solid form is shown in Fig.(4-a), the corresponding PA spectra of RhB are shown in Fig.(4-b) and for CV in Fig.(4-c). The

figures show that the spectra in the case of solid samples exhibit the regular red shift due to dye aggregates.

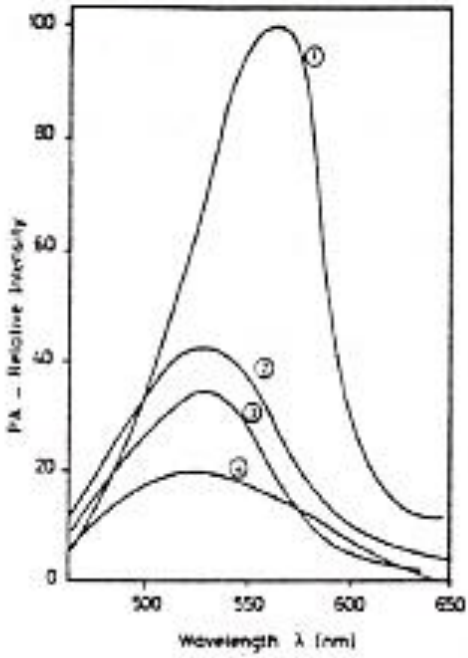

Fig.4a The normalized PAS spectrum of Rh6G in its solid state (1), in ethanol 10^{-2} M/L (2), 0.5 x 10^{-2} M/L (3) and 10^{-3} M/L (4).

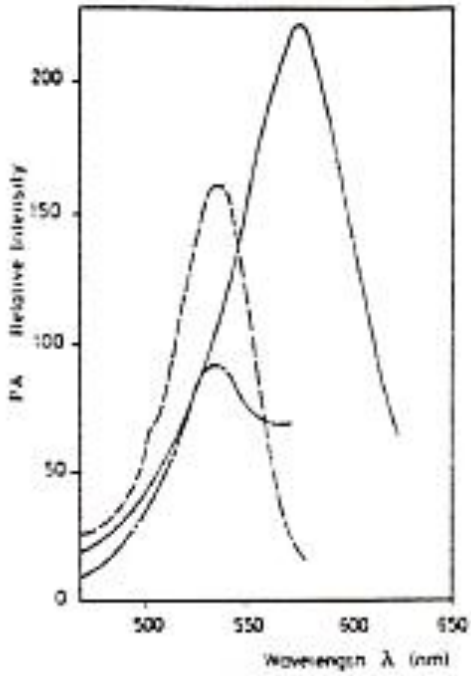

Fig.4b The normalized PAS spectrum of RhB in its solid state (1) and in ethanol 10^{-3} M/L (2), 10^{-2} M/L.

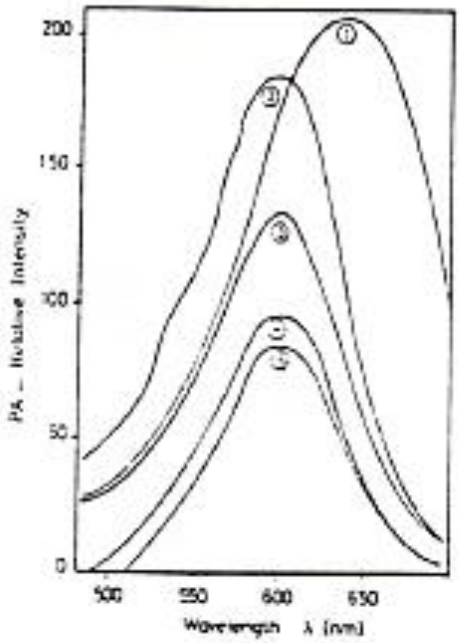

Fig.4c The normalized PAS spectrum of CV in its solid state (1) and in ethanol 0.8 x 10^{-2} M/L (2), 0.6 x 10^{-2} M/L (3), 0.4 x 10^{-2} M/L (4) and 0.2 x10^{-3} M/L (5).

Concentration dependence studies show that, for the same concentration and similar experimental conditions, RhB gives a higher PAS signal than Rh6G. This is expected because fluorescence efficiency in RhB is 40% at 25°C whereas it is 90% for Rh6G [16], hence the PA signal would have then a corresponding reverse ratio nearly 1 : 2.

3- The dependence of the amplitude of the photoacoustic signal on the chopping frequency

Fig (5) shows the experimental results of the variation of the amplitude of the PA signal of the carbon black sample versus the chopper frequencies. It is seen that for low light modulation frquencies there is an increase of the amplitude of the photoacoustic signal.

There is an agreement with the theoretical which can be illustrated in equation (19). Since our sample is a carbon black sample in this case, we should follow the optically opaque, thermally thick conditions, which is the case where the thermal diffusion length is much smaller than the length of sample, but larger than the optical penetration depth. One has $\mu_\beta << \ell$, and $\mu_s < \ell$; $\mu_s > \mu_\beta$ if we set in equation (19) $\exp(-\sigma_s \ell) \cong 0$, $\exp(-\beta \ell) = 0$ and $|r| > 1$, we obtain

$$Q = \frac{(1-i)}{2a_g}\left(\frac{\mu_s}{K_s}\right) y \qquad (20)$$

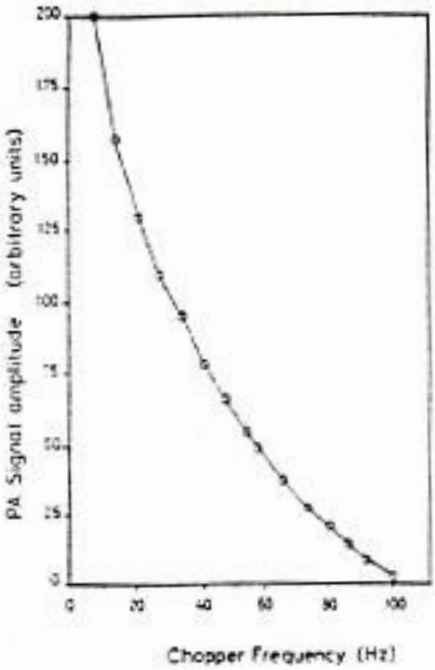

Fig.5 PA signal amplitude as a function of the modulation frequency for a carbon black sample.

Equation (20) tells us that the amplitude of the acoustic signal varies as ω^{-1}. This is in agreement with the experimental results.

From our own studies and other authors, one can conclude that PAS is a good and simple tool to study deexcitation processes of liquids and solids in bulk or film forms. Furthermore, PA response depends upon both the optical and thermal characteristics of the sample, and hence, quantitative thermal analysis for certain samples e.g. thin films [17] could be studied using this technique. The technique becomes particularly useful for sample where the regular optical absorption studies can not be used, as in the case of powdered samples.

Acknowledgment:

The author would like to express her deepest appreciation to Prof. H. Talaat for stimulating discussions.

References:

1. **A. Rosencwaig;** Phys. Today 28(9), 23 (1975).
2. **A. Rosencwaig;** Anal. Chem. 47(6), 592A (1975).
3. **A. Rosencwaig;** Rev. Sci. Instrum. 48, 1133 (1977).
4. **A.A. King and G.E. Kirkbright;** Lab. Practice 23, 377 (1976).
5. **D.M. Monroe and H.S. Reichard;** Am. Lab. 9(2), 119 (1977).
6. **W.R. Harehbarger and M.B. Robin;** Acc. Chem. Res. 6, 329 (19763).
7. **A. Rosencwaig;** in Optoacoustic Spectroscopy and Detection, edited by Yoh-Han Pao (Academic, New York, (1977) p.193 ff).
8. **A. Rosencwaig;** in Advanced in Electronics and Electron Physics, edited by L. Marton (Academic, New York, (1978) Vol. 46 p.207 ff).
9. **J. Tyndall;** Proc. R. Soc. London 31, 307 (1881).
10. **W.C. Roentgen;** Philos. Mag. 11, 510 (1881).
11. **A. Rosencwaig;** Opt. Commun. 7, 305 (1973).
12. **A. Rosencwaig;** Science 181, 657 (1973).
13. **A. Rosencwaig and S.S. Hall;** Anal. Chem. 47, 598 (1975).
14. **A. Rosencwaig and A. Gersho;** J. App. Phys. 47, 64 (1976).
15. **A. Rosencwaig and A. Gersho;** J. App. Phys. 49, 2905 (1978).
16. **J.E. Selvyn and J.I. Steinfeld;** "Aggregation Equilibria Xanthene Dyes", J. Phys. Chem. 76, 762 (1972) and references therein.
17. **Sohair Negm and Hassan Talaat;** Proc. Ultrasonic Symp. Vol.1, 509 (1992).